getting the mos
from your elect

Garth Wi
6 June 2

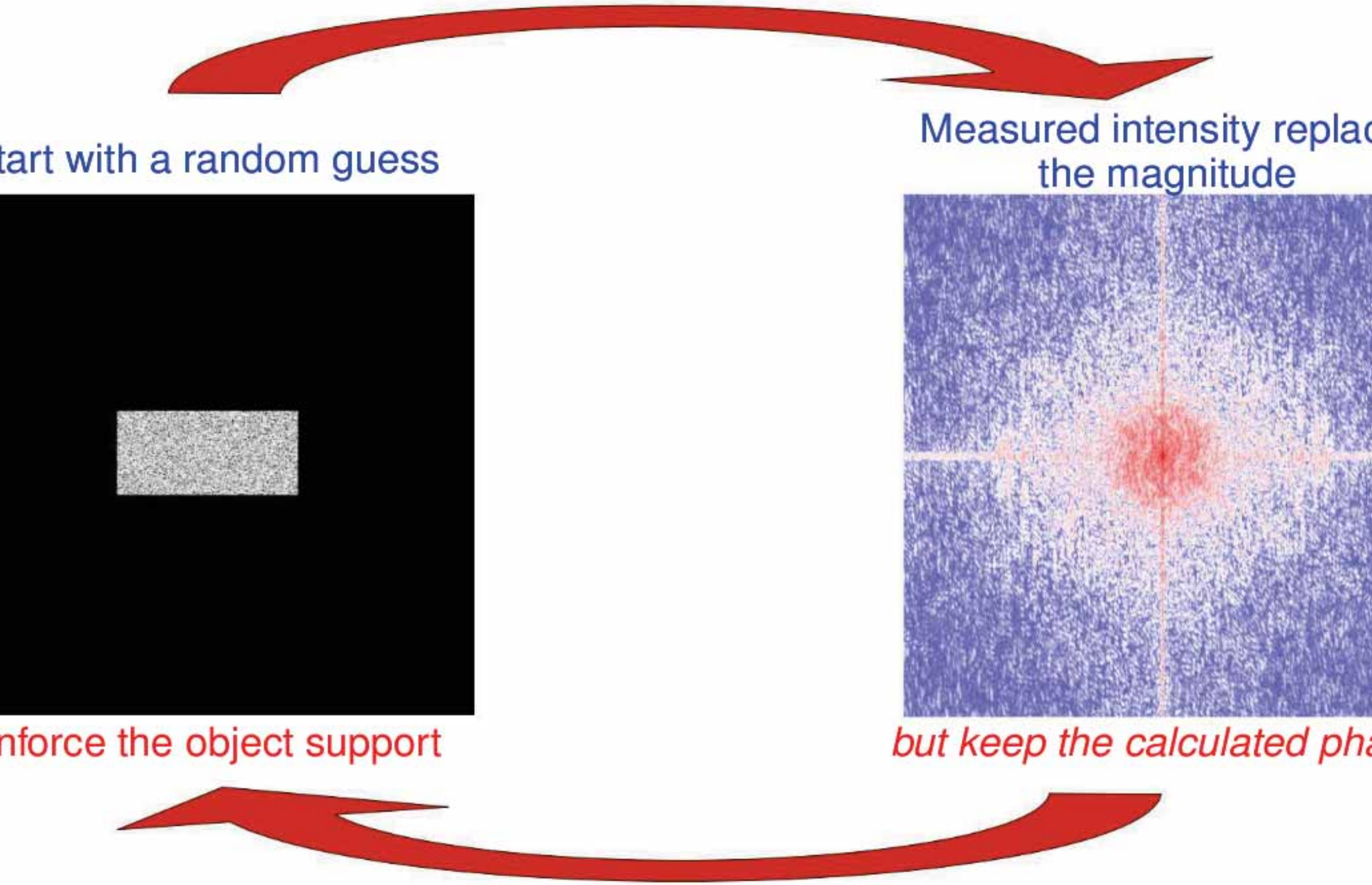
tart with a random guess
Measured intensity replac
the magnitude
nforce the object support
but keep the calculated pha

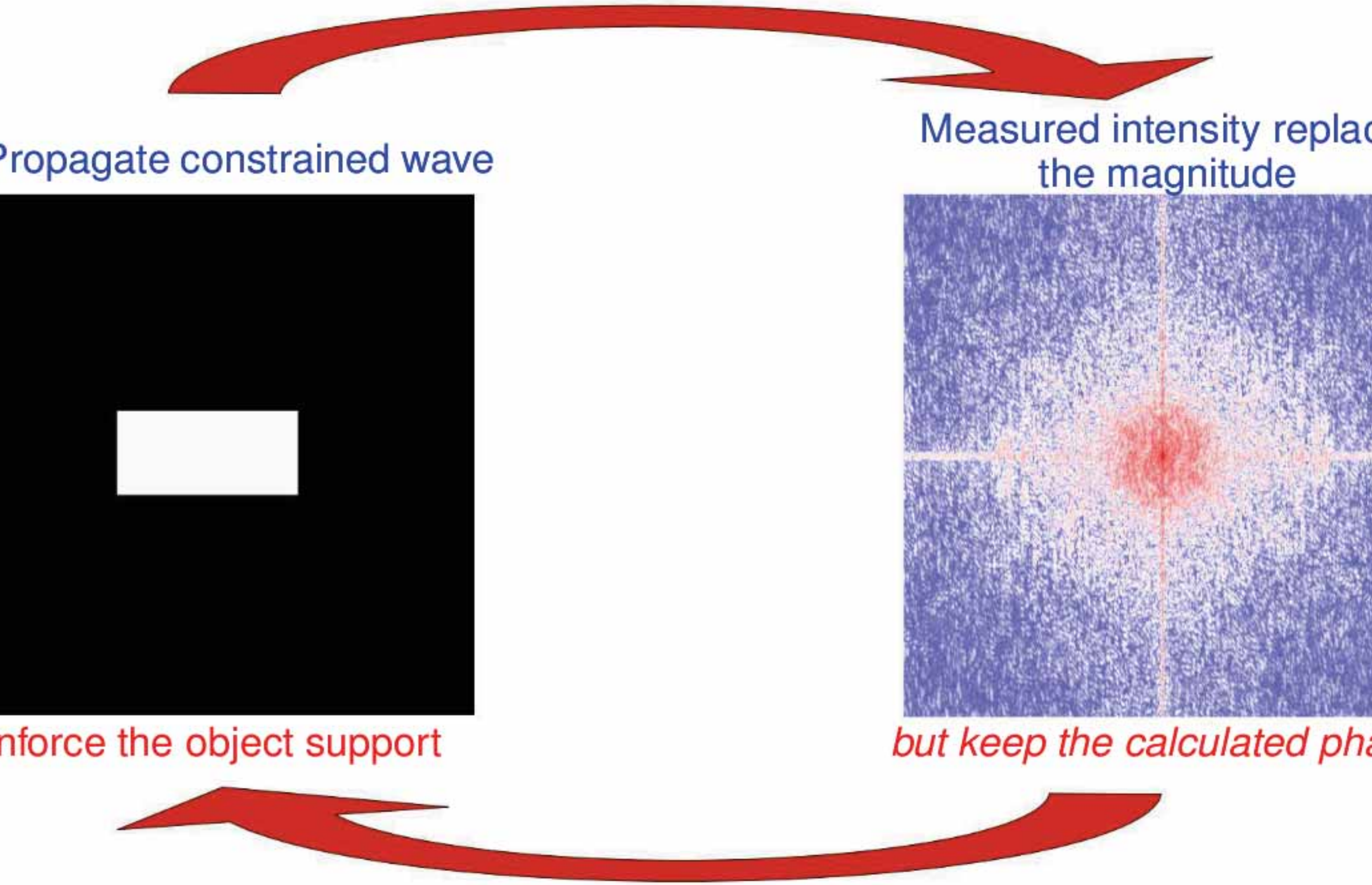

ropagate constrained wave
Measured intensity replac
the magnitude
nforce the object support
but keep the calculated ph

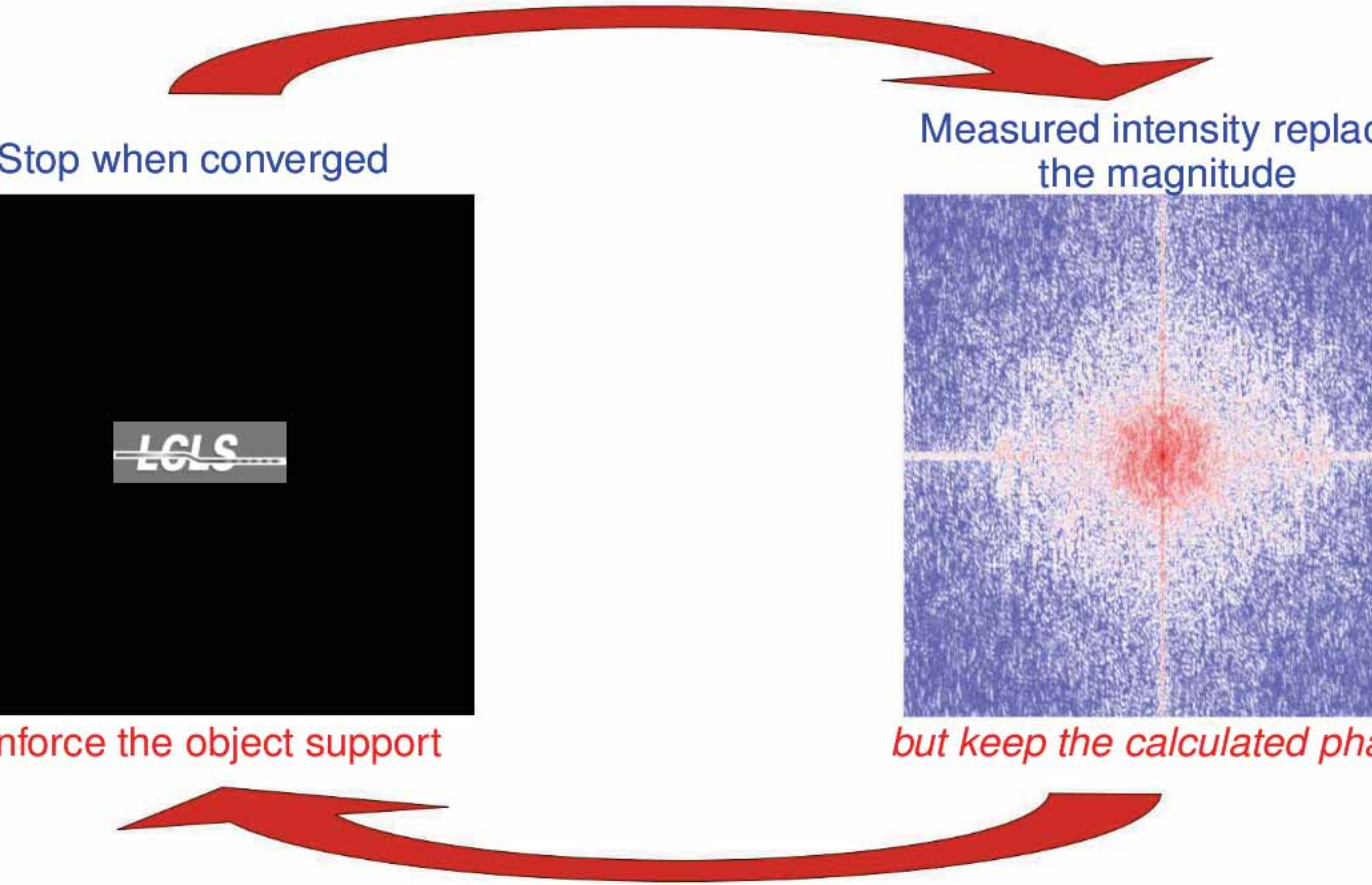
Stop when converged
Measured intensity replac
the magnitude
LCLS
nforce the object support
but keep the calculated pha

retrieval algorithms: a comparison

APPLIED OPTICS / Vol. 21 / 2758 / 1982

p

Iterative algorithms for phase retrieval from intensity data are compared to gradient search methods. Both the problem of phase retrieval from two intensity measurements (in electron microscopy or wave front sensing) and the problem of phase retrieval from a single intensity measurement plus a non-negativity constraint (in astronomy) are considered, with emphasis on the latter. It is shown that both the error-reduction algorithm for the problem of a single intensity measurement and the Gerchberg-Saxton algorithm for the problem of two intensity measurements converge. The error-reduction algorithm is also shown to be closely related to the steepest-descent method. Other algorithms, including the input–output algorithm and the conjugate-gradient method, are shown to converge in practice much faster than the error-reduction algorithm.

Soc. Am. A/Vol. 4, No. 1/January 1987

J. R. Fienup

Rev. Sci. Instrum. **78**, 011301 (2007); doi:10.1063/1.2403783 (*10 pages*)

Invited Article: A unified evaluation of iterat projection algorithms for phase retrieval

S. Marchesini
Lawrence Livermore National Laboratory, 7000 East Avenue, Livermore, California 94550-923
Biophotonics Science and Technology, University of California, Davis, 2700 Stockton Boulevar
Sacramento, California 95817

etrieval by iterated projections

. 20, Issue 1, pp. 40-55 (2003) doi:10.1364/JOSAA.20.000040

Extending the methodology of X-ray crystallography to allow imaging of micrometre-sized non-crystalline specimens

Jianwei Miao*, Pambos Charalambous†, Janos Kirz*
& David Sayre*‡

* *Department of Physics and Astronomy, State University of New Y*
Stony Brook, New York 11794-3800, USA
† *Kings College, Strand, London WC2R 2LS, UK*

High-resolution *ab initio* three-dimensional x-ray diffraction microscopy

Henry N. Chapman, Anton Barty, Stefano Marchesini, Aleksandr Noy, and Stefan P. Hau-Riege

University of California, Lawrence Livermore National Laboratory, 7000 East Avenue, Livermore, California 94550

Congwu Cui, Malcolm R. Howells, and Rachel Rosen

Advanced Light Source, Lawrence Berkeley National Laboratory, 1 Cyclotron Road, Berkeley, California 94720

Haifeng He, John C. H. Spence, and Uwe Weierstall

Department of Physics and Astronomy, Arizona State University, Tempe, Arizona 85287-1504

Tobias Beetz, Chris Jacobsen, and David Shapiro

Department of Physics and Astronoı

Received August 26, 2005; revised October 14,

Coherent x-ray diffraction microscopy is
ited, in principle, by only the wavelengtl
fraction imaging with high resolution in
reconstructed volume images. These imag
a priori knowledge about the shape or cor
a nonperiodic object. We also construct tw
focus (without loss of transverse spatial r
rials science samples at high resolution
used in atomic-resolution ultrafast imag
America

OCIS codes: 340.7460, 110.1650, 110.6

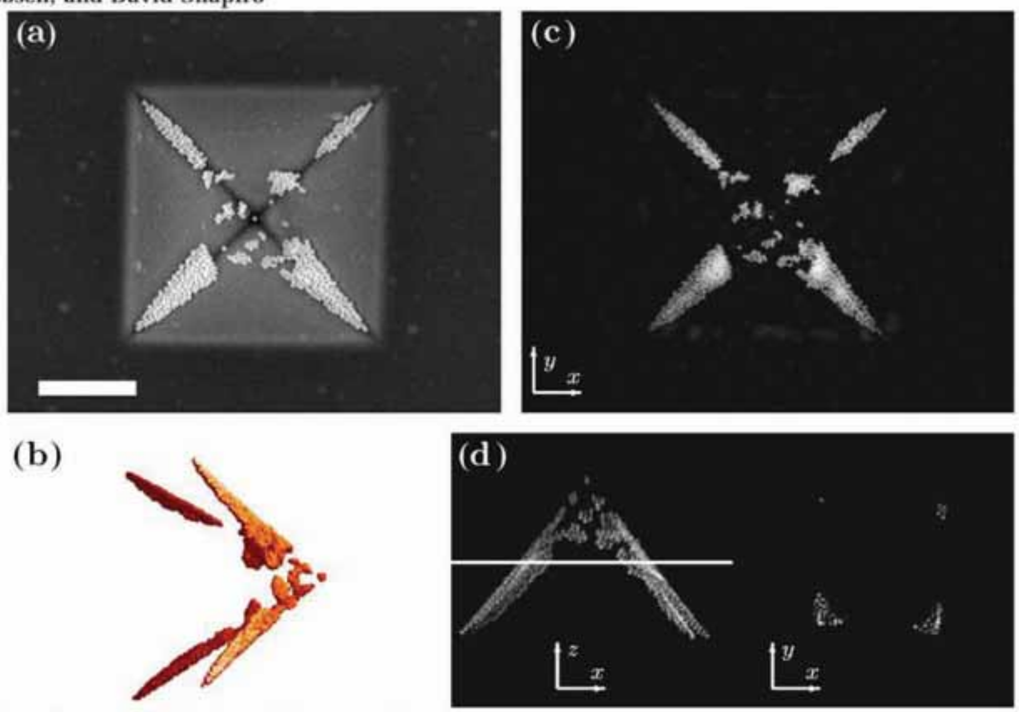

Fig. 2. (Color online) (a) SEM image of the pyramid test object, consisting of 50-nm-diameter gold spheres lining the inside of a pyramid-shaped indentation in a 100-nm-thick silicon nitride membrane. The membrane extends over a window of size 50 μm $\times$1.7 mm, the pyramid base width is 2.5 μm, and the height is 1.8 μm. (b) Isosurface rendering of the reconstructed 3D image. (c) Extremely large depth-of-field x-ray projection image from a central section of the 3D diffraction data set, reconstructed with the Shrinkwrap algorithm. (d) Maximum value projection of the 3D reconstructed image (left) with a horizontal white line indicating the location of a tomographic slice (right). The scale-bar length is 1 μm and applies to all images.

Vol 442|6 July 2006|doi:10.1038/nature04867 nature

LETTERS

Three-dimensional mapping of a deformation field inside a nanocrystal

Mark A. Pfeifer[1]†, Garth J. Williams[1]†, Ivan A. Vartanyants[1]†, Ross Harder[1] & Ian K. Robinson[1]†

PHYSICAL REVIEW B **76**, 115425 (2007)

Orientation variation of surface strain

R. Harder,[1] M. A. Pfeifer,[2] G. J. Williams,[3] I. A. Vartaniants,[4] and I. K. Robinson[1]
[1]*London Center for Nanotechnology, Department of Physics and Astronomy, University College, London WC1E 6l*
[2]*Department of Physics, La Trobe University, Victoria 3086, Australia*
[3]*School of Physics, University of Melbourne, Victoria 3010, Australia*
[4]*HASYLAB, DESY, Notkestrasse 85, D-22607 Hamburg, Germany*
(Received 2 July 2007; published 20 September 2007)

Expansion of the surface layers of a facetted hemispherical nanocrystal of Pb is reported at a temp just below the melting point. Inversion of the coherent x-ray diffraction pattern yields quantitative dimensional maps of the deformation of the crystal from its equilibrium lattice spacing. Most of the sur the crystal has a clear outward displacement, which decays exponentially into the bulk. This is suppre the (111) facet itself and is stronger on the spherical regions, suggesting that it arises from the orien variation of the underlying surface stress.

DOI: 10.1103/PhysRevB.76.115425 PACS number(s): 61.46.Hk, 62.25.+g, 68.35.Gy, ‹

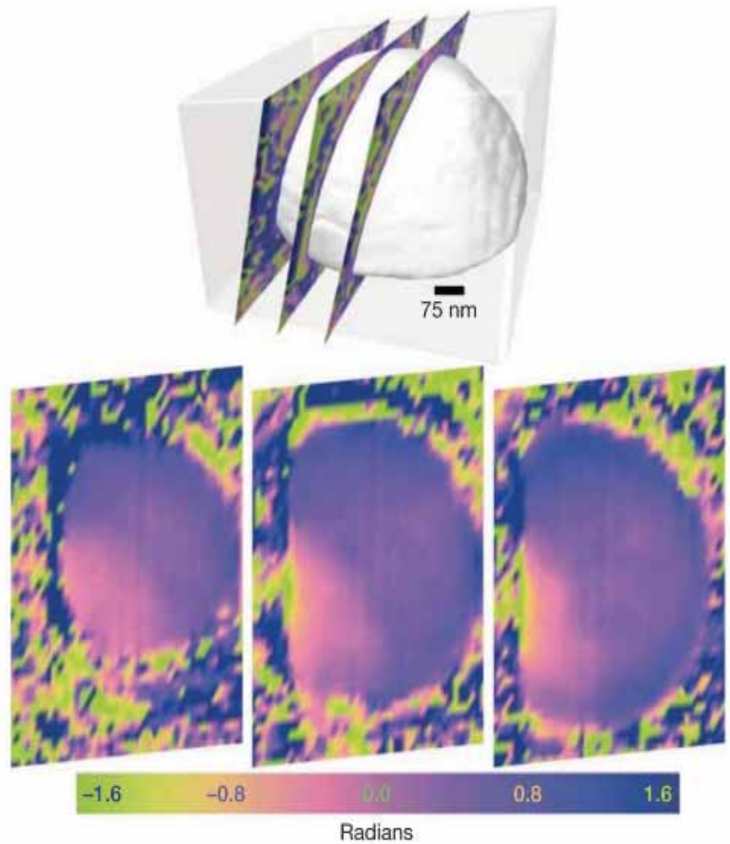

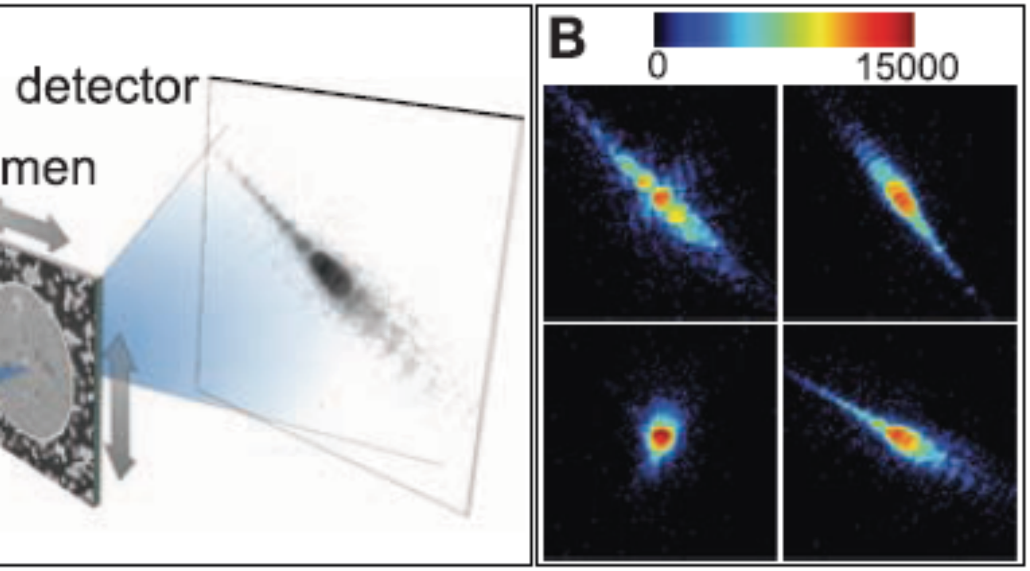

n past the specimen, thereby removing the need

tive biological imaging by ptychographic ffraction microscopy

yer[a,1], Pierre Thibault[b], Sebastian Kalbfleisch[a], André Beerlink[a], Cameron M. Kewish[c], Martin eiffer[b], and Tim Salditt[a,1]

ysik, Georg-August-Universität Göttingen, Friedrich-Hund-Platz 1, 37077 Göttingen, Germany; [b]Department Physik (E17), München, James-Franck-Straße, 85748 Garching, Germany; and [c]Paul Scherrer Institut, 5232 Villigen PSI, Switzerland

High-Resolution Scanning X-ray Diffraction Microscopy

Pierre Thibault,[1]* Martin Dierolf,[1] Andreas Menzel,[1] Oliver Bunk,[1] Christian David

Coherent diffractive imaging (CDI) and scanning transmission x-ray microscopy popular microscopy techniques that have evolved quite independently. CDI pro resolutions below 10 nanometers, but the reconstruction procedures put stringen data quality and sample preparation. In contrast, STXM features straightforward its resolution is limited by the spot size on the specimen. We demonstrate a ptych method that bridges the gap between CDI and STXM by measuring complete di at each point of a STXM scan. The high penetration power of x-rays in combina high spatial resolution will allow investigation of a wide range of complex mes material science specimens, such as embedded semiconductor devices or cellula

SCIENCE VOL 321 18 JULY 2008

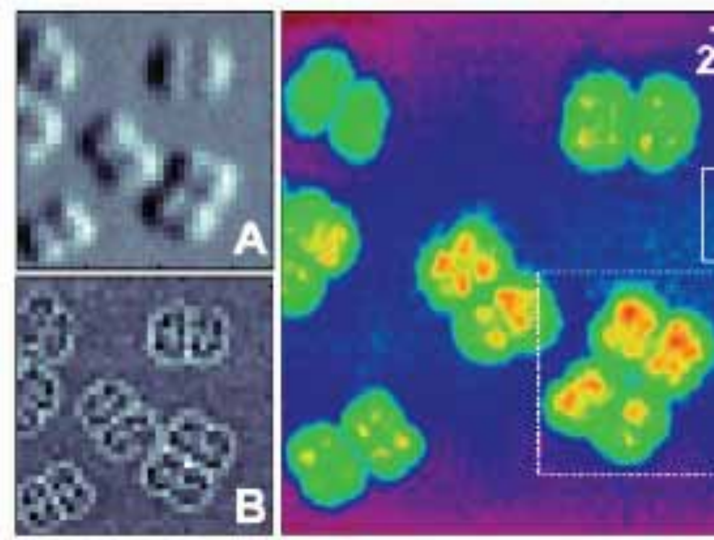

Fig. 2. Ptychographic diffractive imaging of freeze-d cells (1-s dwell time). (*A*) Differential phase contrast i the scanned region. One pixel corresponds to one sca 400×400 nm^2). (*B*) Dark-field contrast image of the sa in *A*. (*C*) PCDI reconstruction of the object transmissio the same region as shown in *A* and *B*. The area marked frame was scanned again in a subsequent scan with long

06) PHYSICAL REVIEW LETTERS week ending 14 JULY 2006

Fresnel Coherent Diffractive Imaging

I. Quiney,[1] B. B. Dhal,[1] C. Q. Tran,[1] K. A. Nugent,[1] A. G. Peele,[2] D. Paterson,[3,*] and M. D. de Jonge[3]

LETTERS

e coherent diffractive imaging

ITH A. NUGENT[1], GARTH J. WILLIAMS[1]*, JESSE N. CLARK[2], ANDREW G. PE

APPLIED PHYSICS LETTERS 93, 214101 (2008)

tive coherent diffractive imaging of an integrated ial resolution of 20 nm

Abbey,[1,a)] Garth J. Williams,[1,a)] Mark A. Pfeifer,[2] Jesse N. Clark,[2] Corey
ela Torrance,[1] Ian McNulty,[3] T. M. Levin,[4] Andrew G. Peele,[2] and Keith A N

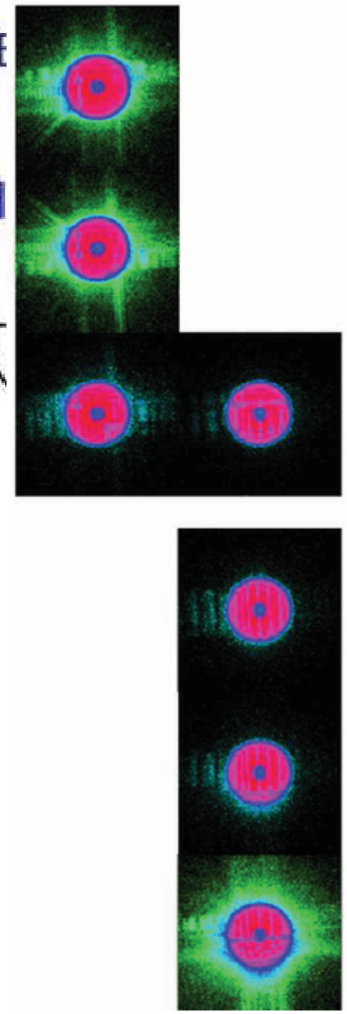

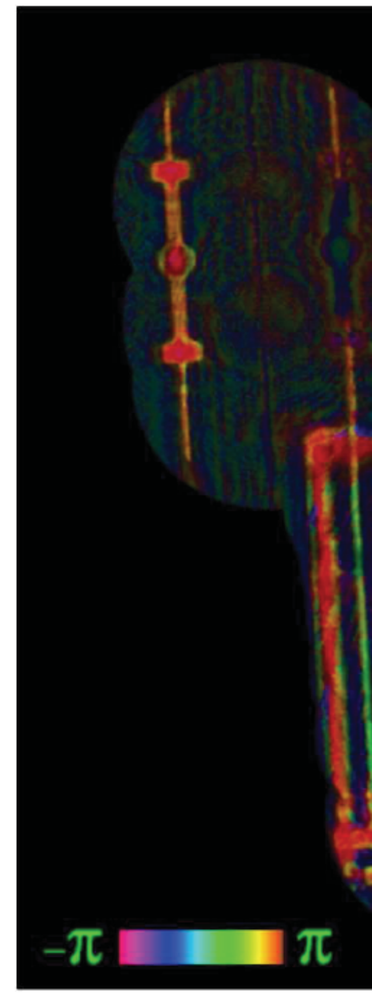

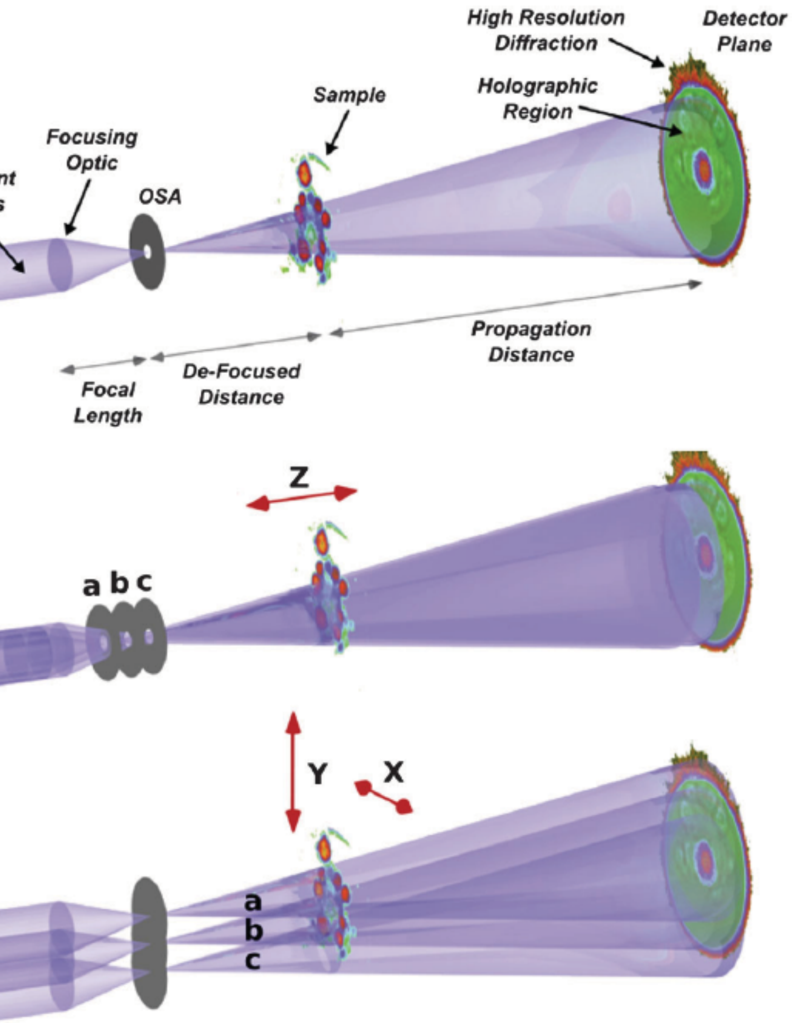

Phase retrieval with transverse translation diversity: a nonlinea optimization approach

Manuel Guizar-Sicairos and James R. Fienup
The Institute of Optics, University of Rochester, Rochester, New York, 1462
mguizar@optics.rochester.edu, fienup@optics.rochester.edu

011) PHYSICAL REVIEW LETTERS week ending 7 JANUARY 201

Diverse Coherent Diffractive Imaging: High Sensitivity with Low Dose

[1,3] Jesse N. Clark,[1,3] David J. Vine,[2,3] Garth J. Williams,[2,3] Mark A. Pfeifer,[1,3] Eugeniu Balaur,[1,3] Ian McNulty,[4] Keith A. Nugent,[2,3] and Andrew G. Peele[1,3,*]
[1]*Department of Physics, La Trobe University, Victoria 3086, Australia*
[2]*School of Physics The University of Melbourne, Victoria 3010, Australia*
[3]*Australian Research Council Centre of Excellence for Coherent X-Ray Science*
Advanced Photon Source, Argonne National Laboratory, Argonne, Illinois 60439, USA

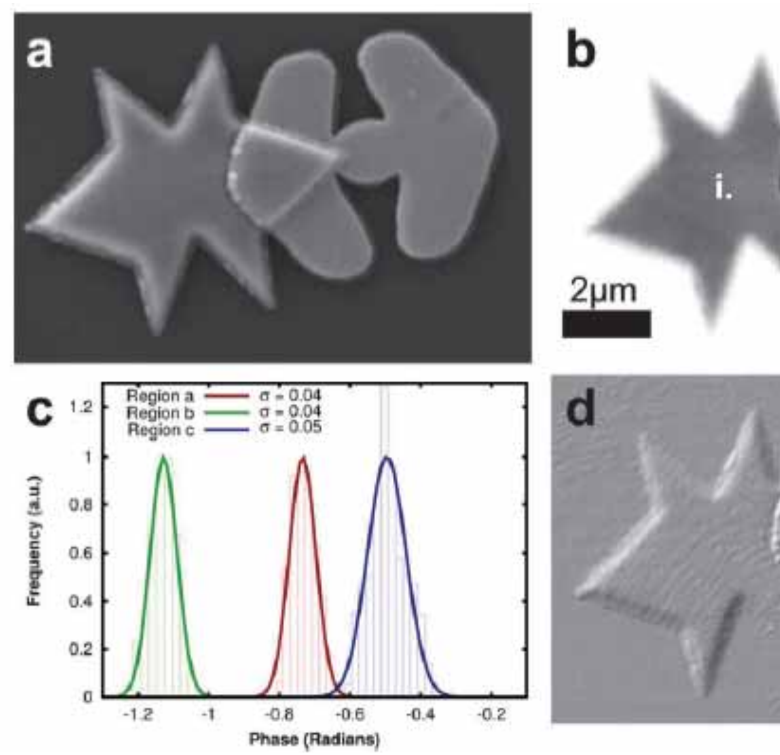

r the past decade, Coherent Imaging ha
en modified by:

- xtending the method to 3D imaging
- tilizing the intensity around Bragg peaks
- sing a "curved wavefront"
- eveloping a scanning geometry
- nducing "diversity" in the experiment and utilizing
resence in the reconstruction

ne of which deals with the source of x-rays!

late, neither third- nor fourth-generation urces produce radiation that meets the ingent requirements of CDI:

- Storage rings (insertion devices) produce illumina with very many coherent modes
- FEL light still has several coherent modes

we exploit explicitly the coherence operties of a source, to what limits and t at advantage?

- an we exploit known coherence properti
  - Yes! This propagation of such light is underst
- hat can we gain?
  - Less beam conditioning
  - Shorter exposure times
- hat's the catch?
  - The detailed properties of the light must be understood

Acknowledgements

ersity of Melbourne

Nugent

Quiney

Vine

Abbey

en

Cadenazzi

n Whitehead

Henderson

LaTrobe University

Andrew Peele

Eugeniu Balaur

Jesse Clark

Corey Putkunz

Australian Synchrotron

David Paterson

Martin De Jonge

Advanced Photon Sourc

Ian McNulty

Funding

The US Department of Energy under contracts governing the APS

The Australian Research Council

ANSTO, under the terms of the ASRP

l measures

$$I(\mathbf{s}) \simeq \int\int \exp[-2\pi i\mathbf{s}\cdot(\mathbf{r_2}-\mathbf{r_1})]J(\mathbf{r_1},\mathbf{r_2})d\mathbf{r_1}d\mathbf{r_2}$$

ere

$$J(\mathbf{r_1},\mathbf{r_2}) = \phi(\mathbf{r_1})\phi^*(\mathbf{r_2})g(\mathbf{r_1}-\mathbf{r_2})$$

he mutual optical intensity depending on two in-plane 2D vectors and

$$g(\mathbf{r_1}-\mathbf{r_2}) = \exp\left(\frac{-|\mathbf{r_1}-\mathbf{r_2}|^2}{2\sigma^2}\right)$$

he coherence function.

wing Wolf, the mutual optical intensity can be rewritten:

$$J(\mathbf{r_1}, \mathbf{r_2}) = \phi(\mathbf{r_1})\phi^*(\mathbf{r_2})g(\mathbf{r_1}, \mathbf{r_2}) = \sum_n \lambda_n \psi_n^*(\mathbf{r_1})\psi_n($$

e ψ_n is a "coherent mode."

$\Longrightarrow$ each mode must obey the support constraint

$\Longrightarrow$ *we can propagate partially coherent scattering!*

Flewett, et al., Opt. Lett. 34, 2198 (200

PRL **103,** 243902 (2009) PHYSICAL REVIEW LETTERS week ending 11 DECEMBER 2009

Diffractive Imaging Using Partially Coherent X Rays

L. W. Whitehead, G. J. Williams, H. M. Quiney, D. J. Vine, R. A. Dilanian, S. Flewett, and K. A. Nugent
School of Physics, The University of Melbourne, Victoria 3010, Australia

A. G. Peele and E. Balaur
Department of Physics, La Trobe University, Bundoora, Victoria 3086, Australia

I. McNulty
Advanced Photon Source, Argonne National Laboratory, 9700 South Cass Avenue, Argonne, Illinois, 60439, USA
(Received 26 August 2009; revised manuscript received 18 November 2009; published 11 December 2009)

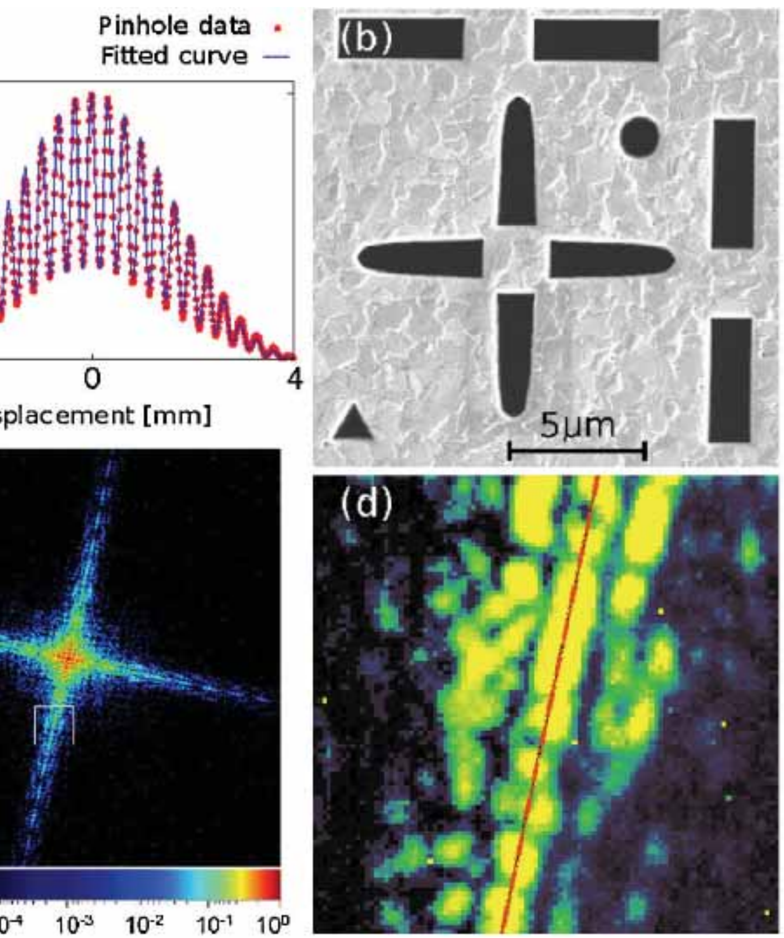

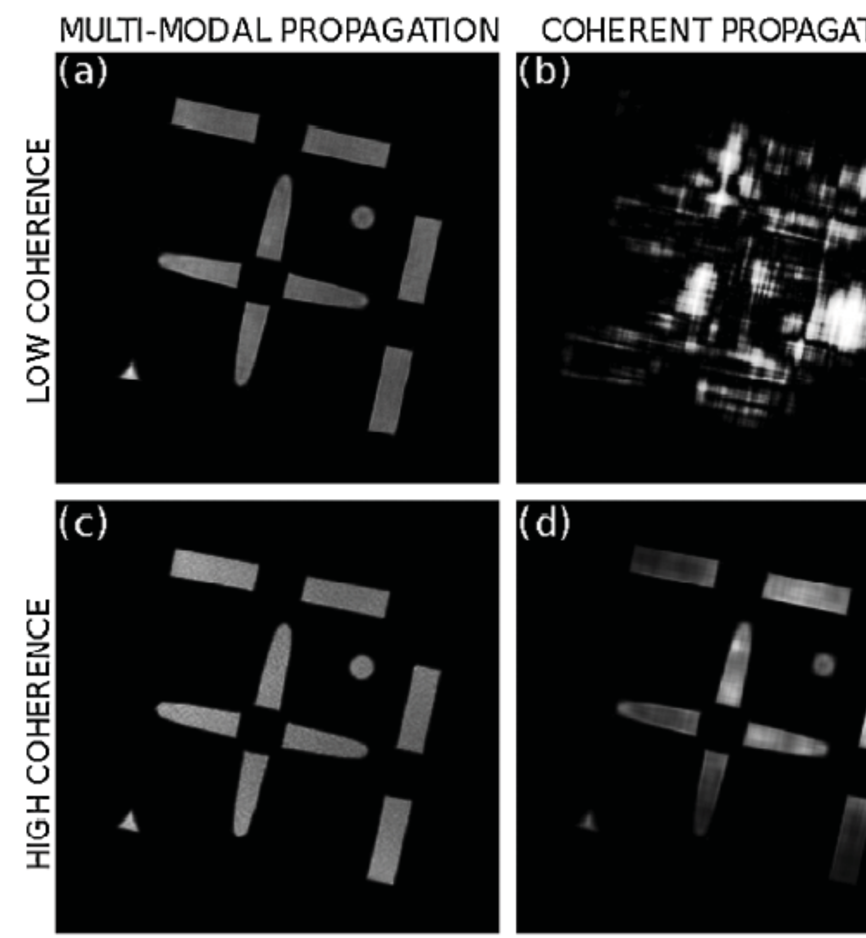

t propagates between two planes according to

$$\psi_\lambda(\mathbf{r}_j, z_j) = -\frac{i}{\lambda z}\exp\left(\frac{2\pi i z_{ij}}{\lambda}\right)\exp\left(\frac{i\pi \mathbf{r}_j^2}{\lambda z_{ij}}\right)\int\int \psi_\lambda(\mathbf{r}_i, z_i)\exp\left(-\frac{2\pi i \mathbf{r}_i \cdot \mathbf{r}_j}{\lambda z_{ij}}\right)d\mathbf{r}_i$$

e, the total intensity in the detector plane can
tten as

$$I(\mathbf{r}_j, \mathbf{z}_j) = \int \xi_\lambda \left|\psi_\lambda(\mathbf{r}_j, \mathbf{z}_j)\right|^2 d\lambda$$

h forms the basis of an algorithmic strategy fo
oad-band illumination CDI!

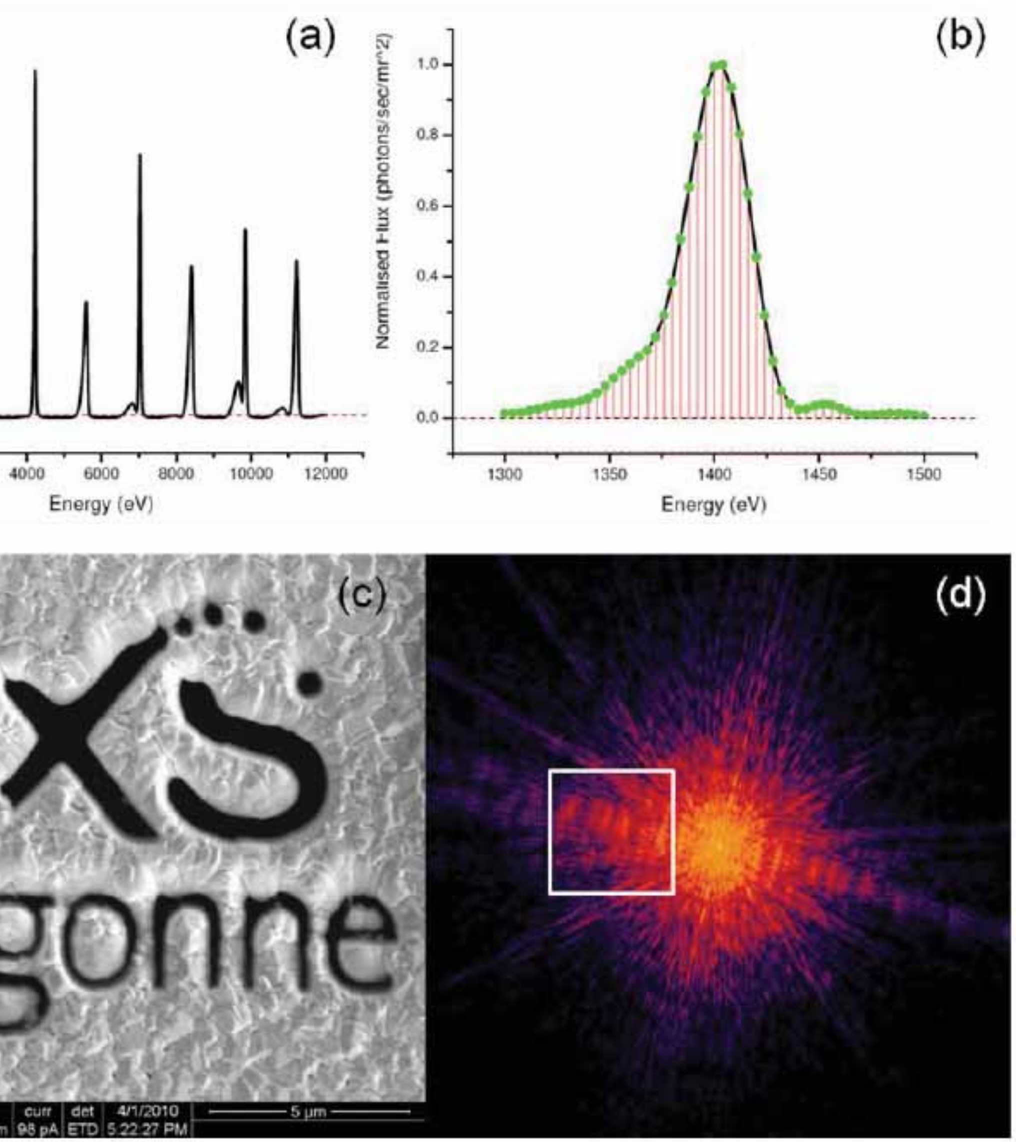

al., accepted by Nature Photonics

- The undulator spectrum is discretised
- A test sample is milled from a Au
- A partially cohere diffraction patterr from the sample

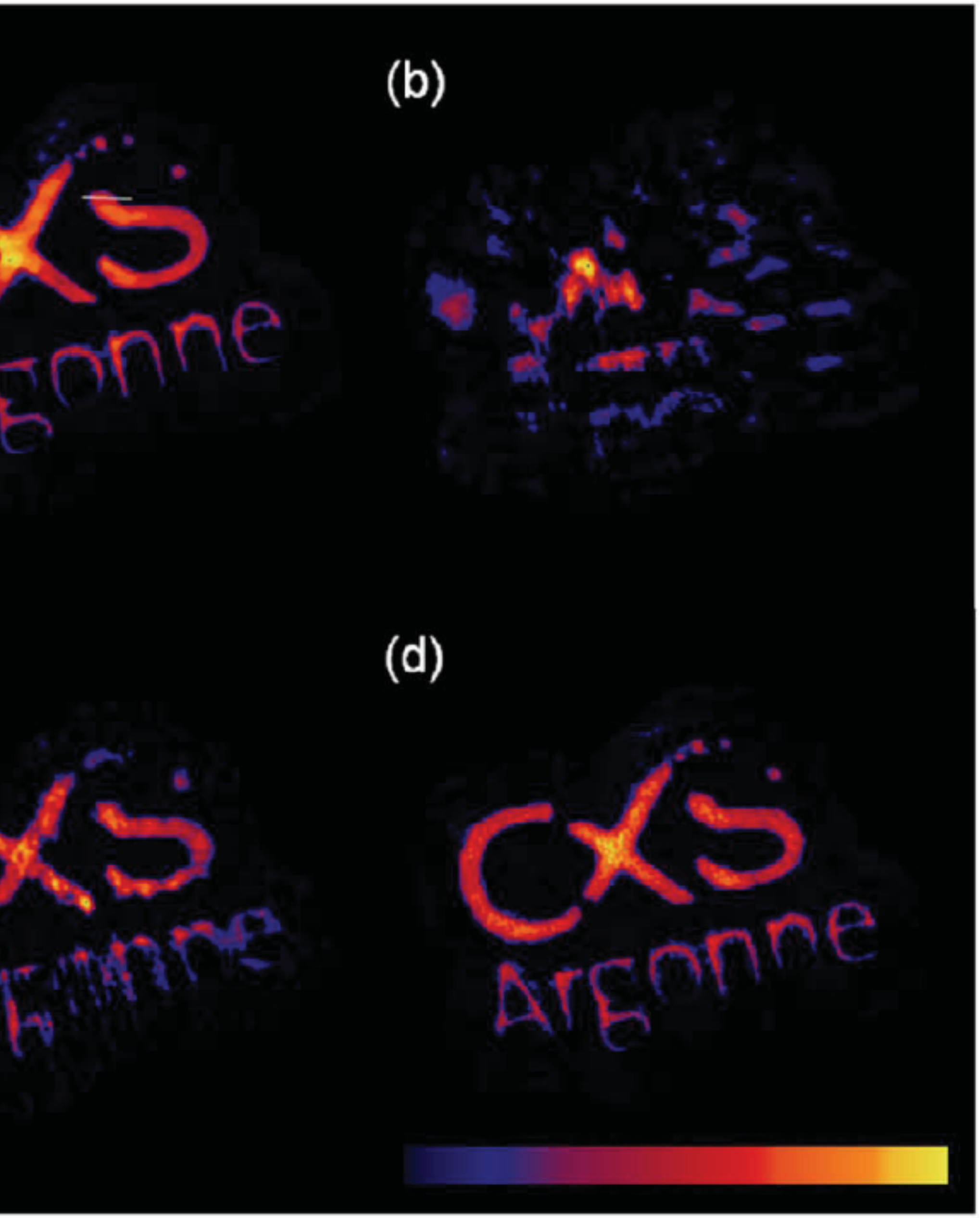

al., accepted by Nature Photonics

- (a) and (d) show that monochromatic and polychromatic CDI ar at the same solution
- Intermediate frames show the consequen of ignoring the partia coherence

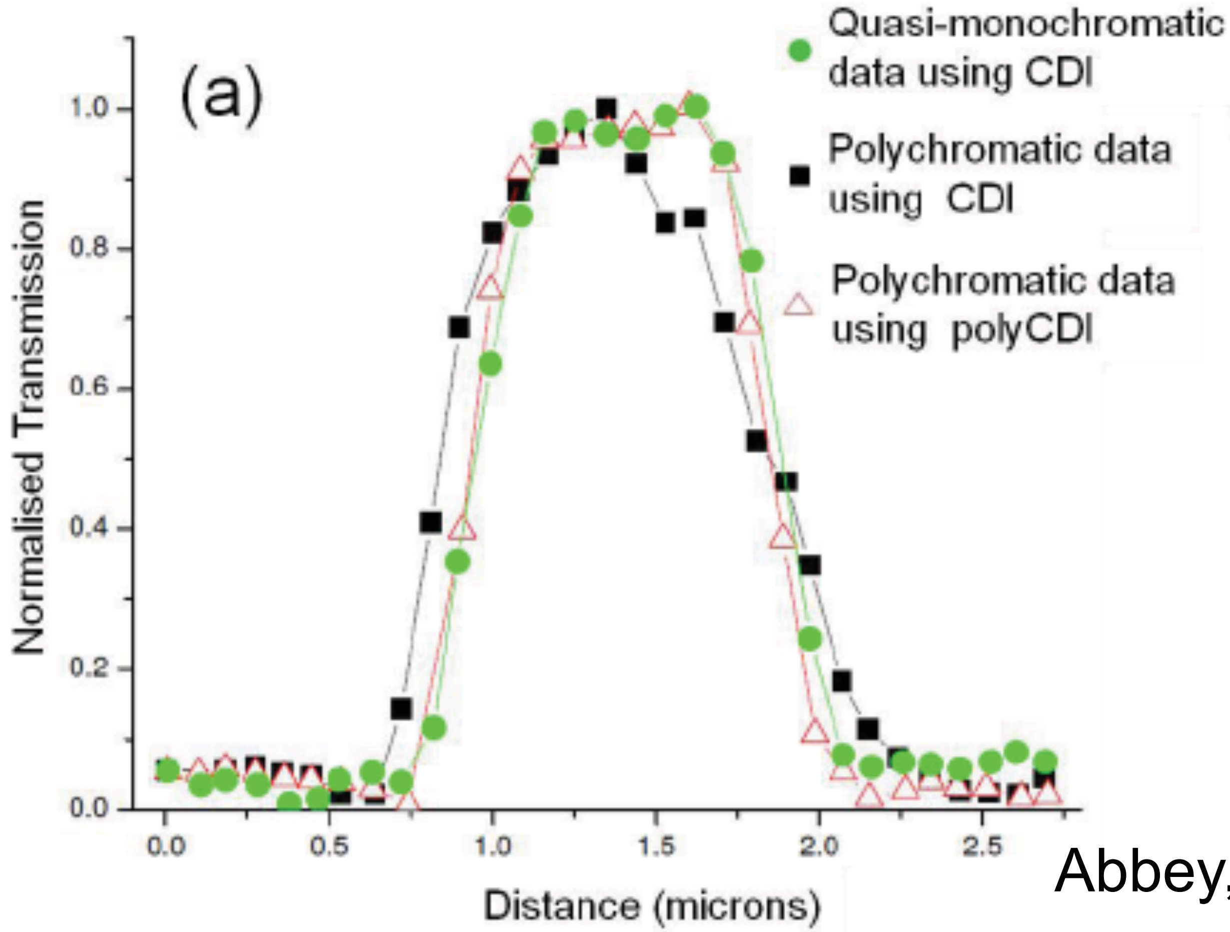

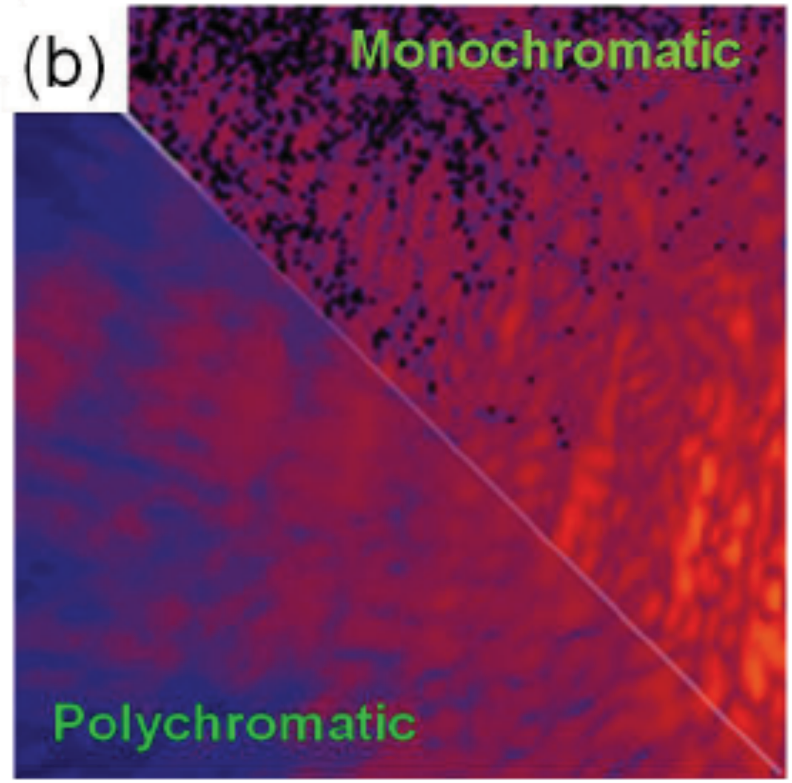

Abbey, et al., accepted by Nature Phot

- omparison of reconstruction fidelity (left)
- aphical depiction of the effect of decreased ngitudinal coherence on the diffraction from the mple

creases acceptable band-width of
umination from ~1% to ~11%

this example, reduces exposure time by
ctor of 60

ansverse coherence can be accomodat
ut limitations very similar to traditional CD

omplicated when the illumination include
sonant edges

DI has made very good progress toward becomin
ernate x-ray microscopy

ere exist may examples of the advantages of
plicitly including characterized beam properties o
mple motions, including algorithmic stability and
tending the method to new samples

e inclusion of the coherence properties of
mination has many potential benefits including: a
duction of the sample exposure time and the
tension of the method to higher x-ray energies

bright, stable source is a huge advantage for CDI

1. An initial guess is made for the sample ESW: $\psi(\mathbf{r}_i, z_i)$.

2. The result is propagated to the far-field via (1) to give the central wavelength distribution $\psi_c(\mathbf{r}_j, z_j)$ and scaled by a factor appropriate to λ_{max} to yield $\psi(\mathbf{r}_j, z_j)_{\lambda_{max}}$.

3. The positions $\mathbf{r}_j$ for the other sampled wavelengths are rescaled according to $\mathbf{r}_j(\lambda_{max} - \Delta\lambda)/\lambda_{max}$.

4. The diffraction patterns from each sampled wavelength are calculated via interpolation onto the new set of points defined by the rescaled values for $\mathbf{r}_j$.

5. The intensity distribution from each pattern is multiplied by a weighting factor determined by the relative contribution of each wavelength to the frequency spectrum: $\xi_\lambda |\psi_\lambda(\mathbf{r}_j, \mathbf{z}_j)|^2$.

6. The sum of the distributions for each sampling point approximates the integral in eq(4) which gives the calculated polychromatic diffraction pattern: $I(\mathbf{r}_j, z_j) = \int \xi_\lambda \left|\psi_\lambda(\mathbf{r}_j, z_j)\right|^2 d\lambda$.

7. The modulus constraint is imposed using: $\left|\psi_c(\mathbf{r}_j, z_j)\right| * \sqrt{I(\mathbf{r}_j, z_j)_{meas}} / \sqrt{I(\mathbf{r}_j, z_j)}$ where $I(\mathbf{r}_j, z_j)_{meas}$ is the measured intensity from experiment.

8. With the amplitude updated, the phase of $\psi_c(\mathbf{r}_j, z_j)$ is retained and the ESW propagated back to the sample plane to give, $\psi(\mathbf{r}_i, z_i)$, after which the support constraint is imposed.

9. Steps 1-9 are repeated and the progress of the reconstruction monitored using an error metric defined as: $\chi^2 = \left(\sqrt{I(\mathbf{r}_{j,} z_j)_{meas}} - \sqrt{I(\mathbf{r}_{j,} z_j)}\right)^2 / I(\mathbf{r}_j, z_j)$.